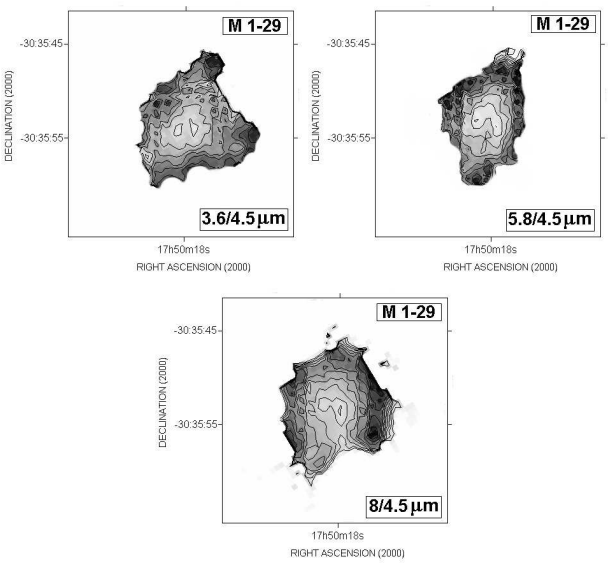

Fig. 18. IRAC band ratio mapping over the projected envelope of M 1-29, where the contour parameters [D, E] are given by [0.2, 0.0930] for 3.6 μm/4.5 μm, [0.5, 0.0669] for 5.8 μm/4.5 μm, and [2.4, 0.0884] for 8.0 μm/4.5 μm. There is evidence for an increase in ratios with radial distance from the nucleus, in conformity with the profiles illustrated in Figure 17.

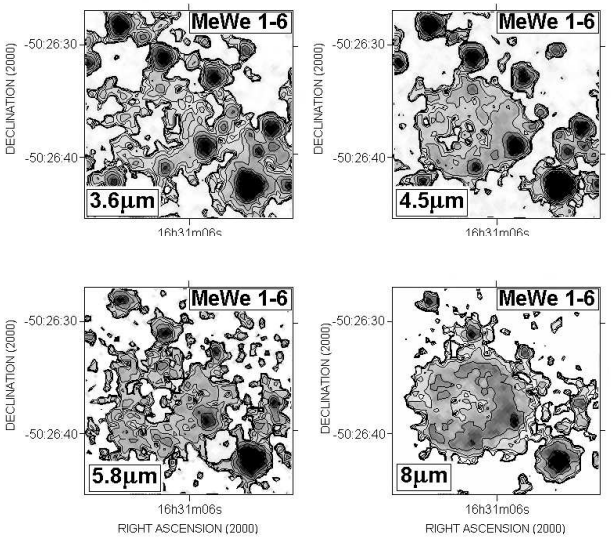

Fig. 19. IRAC mapping of MeWe 1-6, where the contour parameters [A, B, C] are given by [2.28, 1.33, 0.1094] at 3.6 μm, [2.0, 1.00, 0.1179] at 4.5 μm, [7.8, 5.83, 0.0528] at 5.8 μm, and [23.0, 19.62, 0.0128] at 8.0 μm. It is clear that the source has a ring-like morphology at 4.5 and 8.0 μm which is closely comparable to that observed in the visible. However, the high field star densities, and low surface brightness of the envelope make it much more difficult to discern at 3.6 and 5.8 μm.

It would therefore appear that we are detecting most of the region defined through optical imaging.

Profiles through the source are illustrated in Figures 22 and 23, from which it is clear that there is a small dip in 8.0 μm emission close to the centre of the minor axis traverse (Figure 23). This may indicate barely resolved evidence for a central, inclined toroidal structure. The fact that this dip is evident 8.0 μm, but absent at shorter wavelengths may arise where 8.0 μm fluxes are enhanced within the toroid – perhaps as a result of warm dust emission or fluorescently or shock excited H_2. The 3.6 and 4.5 μm fluxes, by contrast, are more likely to arise from ionic transitions, and to trace components of gas within the limits of this structure.

The IRAC band ratios in the lower panels are highly variable with relative position, and show evidence for lower 8.0 μm/4.5 μm and 5.8 μm/4.5 μm ratios close to the centre of the source. These trends are also evident in our contour mapping in Figure 24, where we see a minimum in 5.8 μm/4.5 μm and 8.0 μm/4.5 μm ratios close to the centre of the source, and larger values towards the periphery. There is a great deal of similarity between the longer wave ratio maps, suggesting that their fragmentary appearance is real, and corresponds to actual variations in the ratios. A similarly high level of complexity is also noted in the 3.6 μm/4.5 μm map, although the central minimum is less strong.

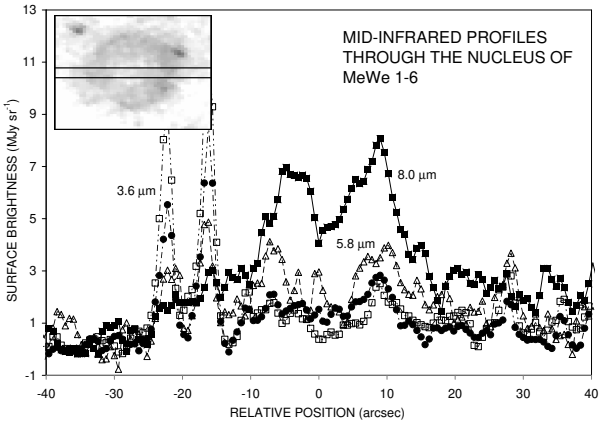

Fig. 20. As for Figure 3, but for profiles through MeWe 1-6. The double-humped structure arises from the ring-like morphology of the source.

3.10. *PN G344.4+01.8 (MPA1654−4041)*

This source was first detected in the MASH II survey, and is quoted as having an elliptical morphology with dimensions $\cong 15 \times 9$ arcsec^2 (Miszalski